Generating Multi-Scroll Chaotic Attractors Via Switching Control

Jinhu Lü[1], Guanrong Chen[2], Xinghuo Yu[3], Henry Leung[4]

[1] Institute of Systems Science, Academy of Mathematics and Systems Science,
Chinese Academy of Sciences, Beijing 100080, China
e-mail: jhlu@mail.iss.ac.cn

[2] Department of Electronic Engineering,
City University of Hong Kong, Hong Kong
e-mail: gchen@ee.cityu.edu.hk

[3] School of Electrical and Computer Engineering,
RMIT University, Melbourne VIC 3001, Australia
e-mail: x.yu@rmit.edu.au

[4] Department of Electrical and Computer Engineering,
University of Calgary, Alberta, T2N 1N4 Canada
e-mail: leungh@enel.ucalgary.ca

Abstract

This paper proposes a new switching control method — saturated function series approach — for generating multi-scroll chaotic attractors. The systematic methodology developed here can create multi-scroll chaotic attractors from a given 3-D linear autonomous system with a saturated function series controller. It includes 1-D $n-$scroll, 2-D $n \times m-$grid scroll, and 3-D $n \times m \times l-$grid scroll chaotic attractors. The chaos generation mechanism in multi-scroll systems is briefly discussed by analyzing the system equilibria.

1 Introduction

Chaos is useful and has great potential in many real-world engineering fields such as in encryption and communications, biomedical engineering, flow dynamics and liquid mixing, power systems protection, etc [1-2]. Recently, we have found that multi-scroll chaotic signals provide the best liquid mixing quality (to be reported soon). Today, the generation of multi-scroll chaotic attractors is no longer a very difficult task [3-16]. Suykens *et al.* introduced several methods for generating $n-$scroll chaotic attractors using simple circuits [3-6,8-9] such as the generalized Chua's circuit [4] and CNN [5]. The essence of these methods is adding breakpoints in the piecewise-linear characteristic of the nonlinear resistor of Chua's circuit [17,18]. They also proposed a stair function method for creating 3-D grid-scroll chaotic attractors [9]. Ozoguz *et al.* presented a nonlinear transconductor approach for generating $n-$scroll attractors [10]. Tang *et al.* introduced a sine-function method for creating $n-$scroll chaotic attractors, with a systematical circuit realization that can physically produce as many as ten scrolls visible on the oscilloscope [7,11]. Lü *et al.* proposed a switching manifold approach for generating chaotic attractors with multiple-merged basins of attraction [12,13]. Hysteresis can also generate chaos [19-25]. Recently, Lü *et al.* presented a hysteresis series method for creating 3-D multi-scroll chaotic attractors [14,15]. Cafagna and Grassi produced a ring of Chua's circuits for generating 3D-scroll chaotic attractors [16]. Elwakil and Kennedy constructed a class of circuit-independent chaotic oscillators [19,20]. They also proposed some hysteresis chaotic oscillators [24]. Note that hysteresis circuit, stair circuit, and saturated circuit are the three kinds of basic circuits. It has been reported that stair circuit and hysteresis circuit can generate 3-D multi-scroll chaotic attractors [9,14,15]. It is interesting to ask whether saturated circuit can also create 3-D multi-scroll chaotic attractors. This paper will give a positive answer to this question.

This paper introduces a new switching control method — saturated function series approach — for generating multi-scroll chaotic attractors, including one-dimensional (1-D) $n-$scroll, two-dimensional (2-D) $n \times m-$grid scroll, and three-dimensional (3-D) $n \times m \times l-$grid scroll chaotic attractors. The chaos generation mechanism in the multi-scroll systems is briefly discussed by analyzing their equilibria. It is noticed that the saturated function series approach developed here

073-40-3016-9 © 2004 ASCC

is different from all methods reported before, such as the stair function method [9] and the hysteresis series approach [14,15]. Firstly, the basic generators are different, which means they have different forming mechanisms. Secondly, the saturated function series is continuous, yet the stair function and hysteresis series are not continuous at some switching points.

This paper is organized as follows. In Section 2, the concept of saturated function series is proposed and some fundamental limited conditions of chaos generation are given for a 3-D linear autonomous system. The saturated function series approach is introduced in Section 3 for creating multi-scroll chaotic attractors, including 1-D $n-$scroll, 2-D $n\times m-$grid scroll, and 3-D $n\times m\times l-$grid scroll attractors, and the chaos generation mechanics of the multi-scroll systems is briefly discussed. Conclusions are finally given in Section 4.

2 Saturated function series

This section reviews the saturated function series concept and presents some fundamental conditions for generating multi-scroll chaotic attractors from a 3-D linear autonomous system using a saturated function series controller.

2.1 Saturated circuit

It is well known that saturated circuit is one of the basic piecewise-linear circuits. The piecewise-linear models for operational amplifiers (op amps) and operational transconductance amplifiers (OTA's) can be well characterized by saturated circuits [26]. Figure 1 shows that the piecewise-linear approximations for op amps and OTA's are quite accurate [26]. It leads to the following representation for op amp, which is in the linear region for $-E_{\text{sat}} \le v_0 \le E_{\text{sat}}$ with voltage amplification A_v, positive saturation E_{sat}, and negative saturation $-E_{\text{sat}}$

$$\begin{cases} v_0 = \frac{A_v}{2}\left(|v_i + \frac{E_{\text{sat}}}{A_v}| - |v_i - \frac{E_{\text{sat}}}{A_v}|\right) \\ i_- = i_+ = 0\,. \end{cases} \tag{1}$$

It is called the op amp finite-gain model. In each of the three regions the op amp can be characterized by a linear circuit.

Similarly, for the OTA, in the linear region $-I_{\text{sat}} \le i_0 \le I_{\text{sat}}$ with transconductance gain g_m, positive saturation I_{sat}, and negative saturation $-I_{\text{sat}}$, one has

$$\begin{cases} i_0 = \frac{g_m}{2}\left(|v_i + \frac{I_{\text{sat}}}{g_m}| - |v_i - \frac{I_{\text{sat}}}{g_m}|\right) \\ i_- = i_+ = 0\,. \end{cases} \tag{2}$$

2.2 Saturated function series

Consider the following saturated function:

$$f_0(x) = \begin{cases} k\,, & \text{if } x > 1 \\ kx\,, & \text{if } |x| \le 1 \\ -k\,, & \text{if } x < -1\,, \end{cases} \tag{3}$$

where $k > 0$ is the slope of the middle segment, the upper radial $\{f_0(x) = k\,|\,x \ge 1\}$ and the lower radial $\{f_0(x) = -k\,|\,x \le -1\}$ are called *saturated plateaus*, and the segment $\{f_0(x) = kx\,|\,|x| \le 1\}$ between the two *saturated plateaus* is called the *saturated slope.* Figure 2 shows the phase portrait of the saturated function $f_0(x)$.

Definition 1: The following piecewise-linear function:

$$f(x;\,k,\,h,\,p,\,q) = \sum_{i=-p}^{q} f_i(x;\,k,\,h) \tag{4}$$

is called a *saturated function series*, where $k > 0$ is the slope of saturated function series, $h > 2$ is the *saturated delay time* of the saturated function series, p and q are positive integers, and

$$f_i(x;k,\,h) = \begin{cases} 2k\,, & \text{if } x > ih+1 \\ k(x-ih)+k\,, & \text{if } |x-ih| \le 1 \\ 0\,, & \text{if } x < ih-1\,, \end{cases}$$

and

$$f_{-i}(x;k,\,h) = \begin{cases} 0\,, & \text{if } x > -ih+1 \\ k(x+ih)-k\,, & \text{if } |x+ih| \le 1 \\ -2k\,, & \text{if } x < -ih-1\,. \end{cases}$$

One can recast the saturated function series $f(x;\,k,\,h,\,p,\,q)$ as follows:

$$f(x;\,k,\,h,\,p,\,q) = \begin{cases} (2q+1)k, & \text{if } x > qh+1 \\ k(x-ih)+2ik, & \text{if } |x-ih| \le 1,\ -p \le i \le q \\ (2i+1)k, & \text{if } \begin{array}{l} ih+1 < x < (i+1)h-1 \\ -p \le i \le q-1 \end{array} \\ -(2p+1)k, & \text{if } x < -ph-1\,. \end{cases} \tag{5}$$

Figure 3 shows the phase portrait of this saturated function series with $k = 1$, $h = 4$. It is noticed that saturated function series (5) is a piecewise-linear continuous function and has better analytical property. However, the stair function in [9] and the hysteresis series in [14,15] are not continuous in switching points.

2.3 Some fundamental limited conditions for chaos generation

Consider the following 3-D linear autonomous system:

$$\begin{cases} \dot{x} = y \\ \dot{y} = z \\ \dot{z} = -a\,x - b\,y - c\,z\,, \end{cases} \tag{6}$$

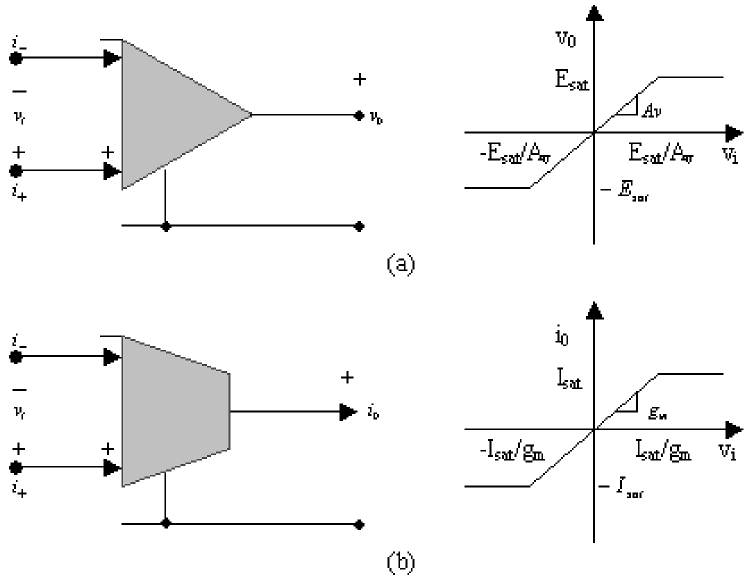

Figure 1. (a) Op amp and its piecewise-linear model; (b) OTA and its piecewise-linear model.

where x, y, z are state variables, and a, b, c are positive real constants. To guide the linear system (6) to generate chaotic behavior, it needs to add a nonlinear controller to stretch and fold the trajectories of the system repeatedly. Note that the piecewise-linear controller is the simplest nonlinear continuous controller. Here, we choose the saturated function series (5) as the controller.

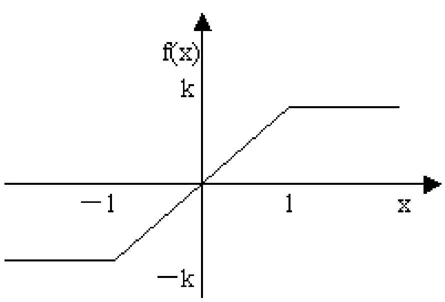

Figure 2. Saturated function $f_0(x)$.

System (6) has a unique equilibrium point (0, 0, 0) and its corresponding characteristic equation is

$$\lambda^3 + c\,\lambda^2 + b\,\lambda + a = 0\,. \qquad (7)$$

Denote $\hat{p} = b - \frac{1}{3}c^2$, $\hat{q} = \frac{2}{27}c^3 - \frac{1}{3}bc + a$, and $\Delta = \frac{ac^3}{27} - \frac{b^2c^2}{108} - \frac{abc}{6} + \frac{b^3}{27} + \frac{a^2}{4}$. Solving Eq. (7) gives

$$\lambda_1 = -\frac{c}{3} + \sqrt[3]{-\frac{\hat{q}}{2} + \sqrt{\Delta}} + \sqrt[3]{-\frac{\hat{q}}{2} - \sqrt{\Delta}}\,, \qquad (8)$$

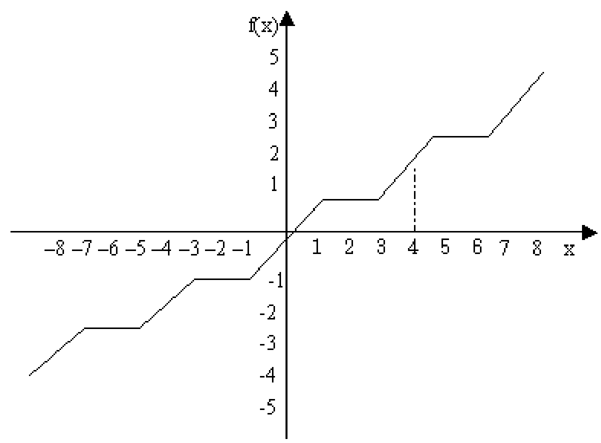

Figure 3. Saturated function series with $k = 1,\ h = 4$.

and

$$\begin{aligned} \lambda_{2,3} &= -\tfrac{c}{3} - \tfrac{1}{2}\left(\sqrt[3]{-\tfrac{\hat{q}}{2} + \sqrt{\Delta}} + \sqrt[3]{-\tfrac{\hat{q}}{2} - \sqrt{\Delta}}\right) \\ &\quad \pm \tfrac{\sqrt{3}}{2}\,i\left(\sqrt[3]{-\tfrac{\hat{q}}{2} + \sqrt{\Delta}} - \sqrt[3]{-\tfrac{\hat{q}}{2} - \sqrt{\Delta}}\right) \\ &\equiv \alpha \pm \beta\, i\,. \end{aligned} \qquad (9)$$

Numerical calculations show that linear system (6) with a saturated function series controller will produce chaotic behavior under the conditions of $\lambda_1 < 0$, $\alpha > 0$, and $\beta \neq 0$. That is, Eq. (7) has a negative eigenvalue and a pair of complex conjugate eigenvalues with positive real parts. Moreover, the equilibrium point (0, 0, 0) is a two-dimensionally unstable saddle, called a *saddle point of index 2* [16,17]. In the following, assume that

$$\begin{aligned}
&\Delta = \tfrac{ac^3}{27} - \tfrac{b^2c^2}{108} - \tfrac{abc}{6} + \tfrac{b^3}{27} + \tfrac{a^2}{4} > 0, \\
&\lambda_1 = -\tfrac{c}{3} + \sqrt[3]{-\tfrac{\hat{q}}{2} + \sqrt{\Delta}} + \sqrt[3]{-\tfrac{\hat{q}}{2} - \sqrt{\Delta}} < 0, \\
&\alpha = -\tfrac{c}{3} - \tfrac{1}{2}\left(\sqrt[3]{-\tfrac{\hat{q}}{2} + \sqrt{\Delta}} + \sqrt[3]{-\tfrac{\hat{q}}{2} - \sqrt{\Delta}}\right) > 0.
\end{aligned} \tag{10}$$

3 Generating multi-scroll chaotic attractors via switching control

This section introduces a new systematic method — saturated function series approach — for generating multi-scroll chaotic attractors, including 1-D $n-$scroll, 2-D $n \times m-$grid scroll, and 3-D $n \times m \times l-$grid scroll chaotic attractors, from the linear autonomous system (6).

3.1 A new double-scroll chaotic attractors

In this subsection, the saturated function $f_0(x)$ is chosen as controller to guide system (6) to create chaos. The controlled system is described by

$$\begin{cases} \dot{x} = y \\ \dot{y} = z \\ \dot{z} = -a\,x - b\,y - c\,z + d_1\,f_0(x)\,, \end{cases} \tag{11}$$

where $f_0(x)$ is defined by (3). When $a = b = c = d_1 = 0.7$, $k = 10$, system (11) has a double-scroll chaotic attractor as shown in Figure 4. Figure 4 (a) shows the x-y plane projection of the double-scroll attractor; Figure 4 (b) shows that the variable $x(t)$ spirals around two values: ± 10, making random excursions between these two values which correspond to the centers of the two scrolls in the attractor.

Obviously, system (11) has three equilibria, $S_\pm\,(\pm 10, 0, 0)$ and $S_0\,(0, 0, 0)$, which correspond to the three piecewise-linear parts of the saturated function $f_0(x)$ in Figure 2, respectively. Equilibria $S_\pm$ has eigenvalues $\lambda_1 = -0.8480$, $\lambda_{2,3} = 0.0740 \pm 0.9055i$, which are called *saddle points of index 2* since the two complex conjugate eigenvalues have positive real parts [16,17]. Equilibrium point S_0 has eigenvalues $\lambda_1 = 1.5309$, $\lambda_{2,3} = -1.1154 \pm 1.6944i$, which is called *saddle point of index 1* since the real eigenvalue is positive [16]. It is noticed that the scrolls are generated only around the equilibria of *saddle points of index 2* [16,17]. Moreover, equilibria $S_\pm$ correspond to the two *saturated plateaus*, which are responsible for generating the two scrolls in the double-scroll attractor. However, the equilibrium point S_0 corresponds to the *saturated slope* and is responsible for connecting these two symmetrical scrolls. The Lyapunov exponent spectrum and Lyapunov dimension can be calculated by the numerical methods described in [27], which are given by $LE_1 = 0.1042$, $LE_2 = 0$, $LE_3 = -0.8043$, and $LD = 2.1297$. According to above analysis, this new double-scroll attractor is similar to but different from Chua's double-scroll attractor [17] since Chua's double-scroll attractor is created by using Chua's circuit.

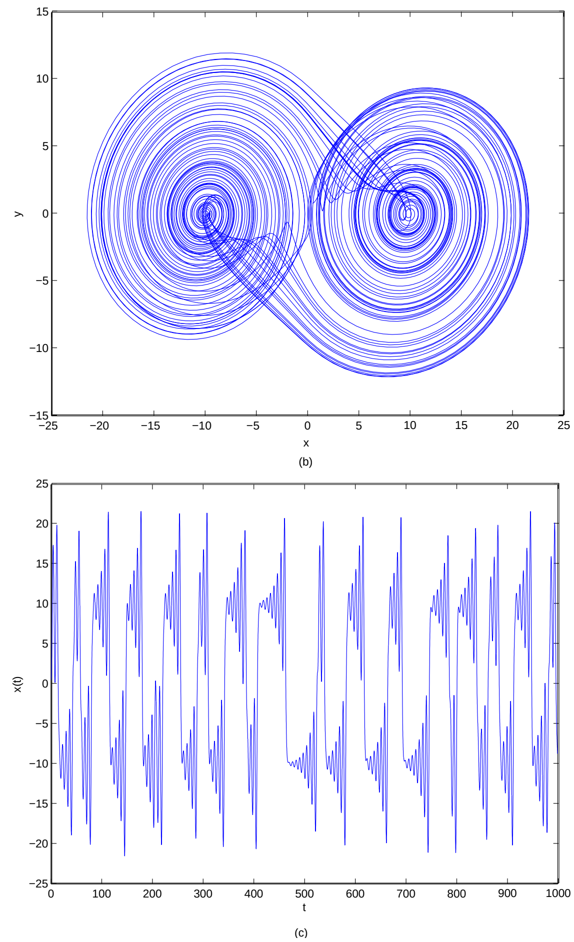

Figure 4. Double-scroll chaotic attractor. (a) x-y plane projection; (b) variable $x(t)$.

3.2 Creating $n-$scroll chaotic attractors

In the following, to create $n-$scroll chaotic attractors ($n \geq 3$), a saturated function series controller is added to system (6), yielding to

$$\begin{cases} \dot{x} = y \\ \dot{y} = z \\ \dot{z} = -a\,x - b\,y - c\,z + d_1\,f(x;\,k_1,\,h_1,\,p_1,\,q_1)\,, \end{cases} \tag{12}$$

where $f(x;\,k_1,\,h_1,\,p_1,\,q_1)$ is defined by (5), and a, b, c, d_1 are positive constants.

Assume that

$$\begin{aligned}
&d_1k_1 > a,\ 2d_1k_1 \geq ah_1,\ \max\{p_1, q_1\}\tfrac{|ah_1 - 2k_1d_1|}{d_1k_1 - a} \leq 1, \\
&(2d_1k_1 - ah_1)(q_1 - 1) < ah_1 - d_1k_1 - a.
\end{aligned} \tag{13}$$

Obviously, all $2(p_1 + q_1) + 3$ equilibrium points of system (12) are located along the x-axis, and can be classified into two different sets:

$$A_x = \left\{-\frac{(2p_1+1)d_1k_1}{a}, \frac{(-2p_1+1)d_1k_1}{a}, \dots, \frac{(2q_1+1)d_1\,k_1}{a}\right\} \tag{14}$$

and

$$B_x = \left\{-\frac{p_1k_1d_1(h_1-2)}{k_1d_1-a}, \frac{(-p_1+1)k_1d_1(h_1-2)}{k_1d_1-a}, \dots, \frac{q_1k_1d_1(h_1-2)}{k_1d_1-a}\right\}. \tag{15}$$

For all equilibria in set A_x, the characteristic equations are Eq. (7) and the corresponding eigenvalues satisfy $\lambda_1 < 0$ and $\lambda_{2,3} = \alpha \pm \beta\, i$ with $\alpha > 0$ and $\beta \neq 0$ from assumption (10). That is, all equilibria in set A_x are *saddle points of index 2*. For all equilibria in set B_x, the corresponding characteristic equations are

$$\lambda^3 + c\,\lambda^2 + b\,\lambda + a - d_1k_1 = 0\,. \tag{16}$$

Since $\lambda_1 + \lambda_2 + \lambda_3 = -c < 0$ and $\lambda_1\lambda_2\lambda_3 = -(a - d_1k_1) > 0$, Eq. (16) has one positive eigenvalue and two negative eigenvalues, or one positive eigenvalue and a pair of complex conjugate eigenvalues with negative real parts. To generate chaos from system (12), one may assume that Eq. (16) has a positive eigenvalue and a pair of complex eigenvalues with negative real parts. It means that all equilibria in set B_x are *saddle points of index 1*. Since the scrolls are generated only around *saddle points of index 2* [16,17], system (12) has the potential to create a maximum of $(p_1 + q_1 + 2)-$scroll chaotic attractor for some suitable parameters a, b, c, d_1, k_1, h_1. It should be emphasized that the $p_1 + q_1 + 2$ equilibria in set A_x are responsible for generating $p_1 + q_1 + 2$ scrolls of the attractor. However, the $p_1 + q_1 + 1$ equilibria in set B_x are responsible for connecting these $p_1 + q_1 + 2$ scrolls to form a whole chaotic attractor. Moreover, each equilibrium point in set A_x corresponds to a unique *saturated plateau* of saturated function series (5) and also corresponds to a unique scroll of the whole attractor. Furthermore, each equilibrium point in set B_x corresponds to a unique *saturated slope* of the saturated function series (5) and also corresponds to a unique connection between two neighboring scrolls.

Figure 6 displays a 6−scroll chaotic attractor of system (12), where $a = b = c = d_1 = 0.7$, $k_1 = 9$, $h_1 = 18$, $p_1 = 2$, $q_1 = 2$. The Lyapunov exponent spectrum of this 6−scroll chaotic attractor includes $LE_1 = 0.1486$, $LE_2 = 0$, $LE_3 = -0.8457$. In fact, system (12) can create an $n-$scroll chaotic attractor ($n \geq 3$), including odd and even scroll chaotic attractor, by adjusting suitable parameters.

3.3 Creating 2D $n \times m-$grid scroll chaotic attractors

In this subsection, a saturated function series controller is added to system (6) for generating $n \times m-$grid scroll

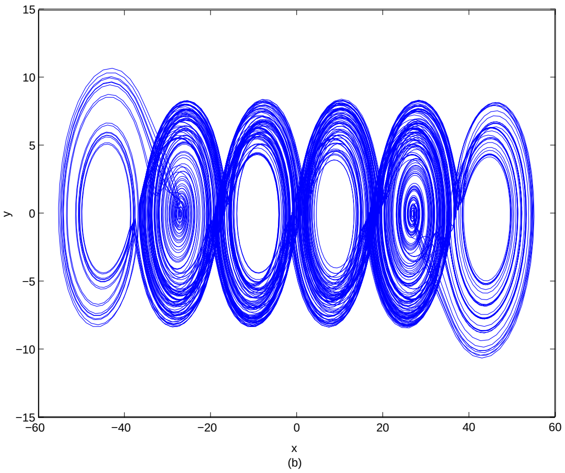

Figure 5. 6−scroll chaotic attractor.

chaotic attractors. The controlled system is described by

$$\left\{\begin{array}{rcl} \dot{x} &=& y - \frac{d_2}{b} f(y;\, k_2,\, h_2,\, p_2,\, q_2) \\ \dot{y} &=& z \\ \dot{z} &=& -a\,x - b\,y - c\,z + d_1\, f(x;\, k_1,\, h_1,\, p_1,\, q_1) \\ && + d_2\, f(y;\, k_2,\, h_2,\, p_2,\, q_2)\,, \end{array}\right. \tag{17}$$

where $f(x;\, k_1,\, h_1,\, p_1,\, q_1)$ and $f(y;\, k_2,\, h_2,\, p_2,\, q_2)$ are defined by (5), and a, b, c, d_1, d_2 are positive constants.

Denote, in addition to (14) and (15), the following:

$$A_y = \left\{-\frac{(2p_2+1)d_2k_2}{b}, \frac{(-2p_2+1)d_2k_2}{b}, \dots, \frac{(2q_2+1)d_2k_2}{b}\right\} \tag{18}$$

and

$$B_y = \left\{-\frac{p_2k_2d_2(h_2-2)}{k_2d_2-b}, \frac{(-p_2+1)k_2d_2(h_2-2)}{k_2d_2-b}, \dots, \frac{q_2k_2d_2(h_2-2)}{k_2d_2-b}\right\}. \tag{19}$$

Assume that (13) holds and

$$d_2k_2 > b,\ 2d_2k_2 \geq bh_2,\ \max\{p_2, q_2\}\frac{|bh_2-2k_2d_2|}{d_2k_2-b} \leq 1, \quad (2d_2k_2 - bh_2)(q_2 - 1) < bh_2 - d_2k_2 - b\,. \tag{20}$$

Then system (17) has $(2p_1 + 2q_1 + 3) \times (2p_2 + 2q_2 + 3)$ equilibrium points, which are located on the x-y plane and given by

$$O_{xy} = \{\,(x^*,\, y^*)\,|\, x^* \in A_x \cup B_x\,,\, y^* \in A_y \cup B_y\,\}\,. \tag{21}$$

It is noticed that all equilibria can be classified into four different sets:

$$\begin{array}{l} A_1 = \{\,(x^*,\, y^*)\,|\, x^* \in A_x\,,\, y^* \in A_y\,\}\,, \\ A_2 = \{\,(x^*,\, y^*)\,|\, x^* \in A_x\,,\, y^* \in B_y\,\}\,, \\ A_3 = \{\,(x^*,\, y^*)\,|\, x^* \in B_x\,,\, y^* \in A_y\,\}\,, \\ A_4 = \{\,(x^*,\, y^*)\,|\, x^* \in B_x\,,\, y^* \in B_y\,\}\,. \end{array}$$

Obviously, the characteristic equations of the linearized system evaluated at the equilibria in set A_1 are Eq. (7) and the corresponding eigenvalues satisfy $\lambda_1 < 0$ and $\lambda_{2,3} = \alpha \pm \beta\, i$ with $\alpha > 0$ and $\beta \neq 0$ by assumption (10). It means that all equilibria in set A_1 are *saddle points of index 2*. For all equilibria in set A_2, the corresponding characteristic equations are

$$\lambda^3 + c\,\lambda^2 + (b - k_2 d_2)\,\lambda + a\left(1 - \frac{k_2 d_2}{b}\right) = 0\,. \quad (22)$$

Since $\lambda_1 + \lambda_2 + \lambda_3 = -c < 0$ and $\lambda_1\lambda_2\lambda_3 = -a(1 - \frac{k_2 d_2}{b}) > 0$, Eq. (22) has one positive eigenvalue and two negative eigenvalues, or one positive eigenvalue and a pair of complex conjugate eigenvalues with negative real parts. Moreover, all equilibria in A_2 are *saddle points of index 1*. For all equilibria in A_3, the corresponding characteristic equations are Eq. (16) and these equilibria are *saddle points of index 1*. Similarly, for all equilibria in A_4, the corresponding characteristic equations are

$$\lambda^3 + c\lambda^2 + (b - k_2 d_2)\lambda + (a - dk_1)\left(1 - \frac{k_2 d_2}{b}\right) = 0. \quad (23)$$

Since $\lambda_1 + \lambda_2 + \lambda_3 = -c < 0$ and $\lambda_1\lambda_2\lambda_3 = -(a - dk_1)(1 - \frac{k_2 d_2}{b}) < 0$, Eq. (23) has one negative eigenvalue and two positive eigenvalues, or three negative eigenvalues, or one negative eigenvalue and a pair of complex conjugate eigenvalues. To create chaos from system (17), one may assume that Eq. (23) has one negative eigenvalue and a pair of complex conjugate eigenvalues with positive real parts. Thus, the equilibria in A_4 are *saddle points of index 2*. Since the scrolls can be generated only around *saddle points of index 2* [16,17], the equilibria in A_1 and A_4 may create scrolls. However, our numerical simulations show that only the equilibria in A_1 can generate scrolls. In fact, having a *saddle point of index 2* is only a necessary condition, but not a sufficient condition for generating scrolls. According to the Homoclinic Šilnikov Theorem [18], it needs a condition — existence of a homoclinic orbit in the neighboring region of the equilibrium point — for generating scrolls. Therefore, system (17) has the potential to create a maximum of 2D $(p_1 + q_1 + 2) \times (p_2 + q_2 + 2)-$grid scroll chaotic attractor, called *2-D $n \times m-$grid scroll* chaotic attractor, for suitable parameters $a, b, c, d_1, d_2, k_1, h_1, k_2, h_2$. Note that each equilibrium point in A_1 corresponds to a unique 2D *saturated plateau* and also corresponds to a unique scroll in the whole attractor. Moreover, other equilibria in A_2, A_3, A_4 correspond to the *saturated slopes* and are responsible for connecting these $(p_1 + q_1 + 2) \times (p_2 + q_2 + 2)$ scrolls.

Figure 6 shows a $6 \times 6-$grid scroll chaotic attractor, where $a = b = c = d_1 = d_2 = 0.7$, $k_1 = k_2 = 50$, $h_1 = h_2 = 100$, $p_1 = q_1 = p_2, = q_2 = 2$. Clearly, there are 6 scrolls in the $x-$direction and 6 scrolls in the $y-$direction, as shown in Figure 6. The Lyapunov exponent spectrum of this $6 \times 6-$grid scroll attractor includes $LE_1 = 0.1599$, $LE_2 = 0$, $LE_3 = -0.8622$. Note that these 2-D $n \times m-$grid scroll chaotic attractors are generated in exactly the same way as the 1-D case discussed in the last subsection, except that the directions of the system trajectories are more vertical here. Similarly, one can design 2-D $n \times m-$grid scroll attractors in x-z or y-z directions.

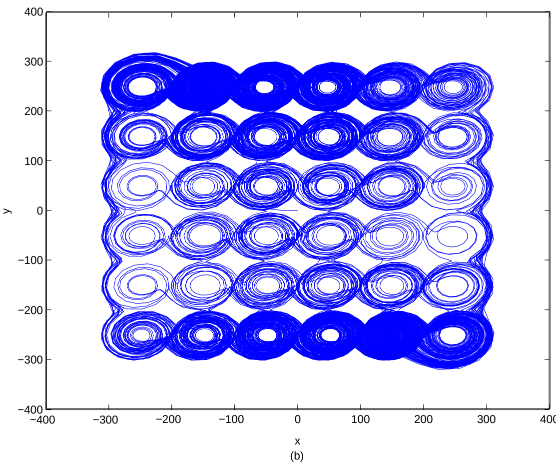

Figure 6. 2-D $6 \times 6-$grid scroll chaotic attractors.

3.4 Creating 3-D $n \times m \times l-$grid scroll chaotic attractors

In this subsection, a saturated function series controller is added to system (6) for creating 3-D $n \times m \times l-$grid scroll chaotic attractors. The controlled system is

$$\left\{\begin{array}{lcl} \dot{x} & = & y - \frac{d_2}{b} f(y;\, k_2,\, h_2,\, p_2,\, q_2) \\ \dot{y} & = & z - \frac{d_3}{c} f(z;\, k_3,\, h_3,\, p_3,\, q_3) \\ \dot{z} & = & -ax - by - cz + d_1 f(x; k_1, h_1, p_1, q_1) \\ & & +d_2 f(y; k_2, h_2, p_2, q_2) + d_3 f(z; k_3, h_3, p_3, q_3), \end{array}\right. \quad (24)$$

where $f(x;\, k_1,\, h_1,\, p_1,\, q_1)$, $f(y;\, k_2,\, h_2,\, p_2,\, q_2)$, and $f(z;\, k_3,\, h_3,\, p_3,\, q_3)$ are defined by (5), and $a,\, b,\, c,\, d_1,\, d_2,\, d_3$ are positive constants.

Denote, in addition to (14), (15), (18), and (19), the following:

$$A_z = \left\{-\frac{(2p_3 + 1)d_3k_3}{c}, \frac{(-2p_3 + 1)d_3k_3}{c}, \cdots, \frac{(2q_3 + 1)d_3k_3}{c}\right\} \quad (25)$$

and

$$B_z = \left\{-\frac{p_3k_3d_3(h_3 - 2)}{k_3d_3 - c}, \frac{(-p_3 + 1)k_3d_3(h_3 - 2)}{k_3d_3 - c}, \dots, \frac{q_3k_3d_3(h_3 - 2)}{k_3d_3 - c}\right\}. \quad (26)$$

Assume that (13) and (20) hold and

$$d_3k_3 > c, 2d_3k_3 \geq ch_3, \max\{p_3, q_3\}\frac{|ch_3 - 2k_3d_3|}{d_3k_3 - c} \leq 1,$$
$$(2d_3k_3 - ch_3)(q_3 - 1) < ch_3 - d_3k_3 - c\,. \quad (27)$$

Then system (24) has $(2p_1+2q_1+3) \times (2p_2+2q_2+3) \times (2p_3+2q_3+3)$ equilibrium points, which are given by

$$O_{xyz} = \{(x^*, y^*, z^*) | x^* \in A_x \cup B_x, \; y^* \in A_y \cup B_y, \; z^* \in A_z \cup B_z\}. \tag{28}$$

Note that all equilibria can be classified into eight different sets:

$$\begin{aligned}
\bar{A}_1 &= \{(x^*, y^*, z^*) \,|\, x^* \in A_x, \; y^* \in A_y, \; z^* \in A_z\}, \\
\bar{A}_2 &= \{(x^*, y^*, z^*) \,|\, x^* \in A_x, \; y^* \in A_y, \; z^* \in B_z\}, \\
\bar{A}_3 &= \{(x^*, y^*, z^*) \,|\, x^* \in A_x, \; y^* \in B_y, \; z^* \in A_z\}, \\
\bar{A}_4 &= \{(x^*, y^*, z^*) \,|\, x^* \in A_x, \; y^* \in B_y, \; z^* \in B_z\}, \\
\bar{A}_5 &= \{(x^*, y^*, z^*) \,|\, x^* \in B_x, \; y^* \in A_y, \; z^* \in A_z\}, \\
\bar{A}_6 &= \{(x^*, y^*, z^*) \,|\, x^* \in B_x, \; y^* \in A_y, \; z^* \in B_z\}, \\
\bar{A}_7 &= \{(x^*, y^*, z^*) \,|\, x^* \in B_x, \; y^* \in B_y, \; z^* \in A_z\}, \\
\bar{A}_8 &= \{(x^*, y^*, z^*) \,|\, x^* \in B_x, \; y^* \in B_y, \; z^* \in B_z\}.
\end{aligned}$$

For all equilibria in A_1, the corresponding characteristic equations are Eq. (7). From assumption (10), all equilibria in A_1 are *saddle points of index 2*. For the equilibrium points in A_2, the corresponding characteristic equations are

$$\lambda^3 + (c - d_3k_3)\lambda^2 + b\left(1 - \frac{k_3d_3}{c}\right)\lambda + a\left(1 - \frac{k_3d_3}{c}\right) = 0. \tag{29}$$

Since $\lambda_1 + \lambda_2 + \lambda_3 = -(c - d_3k_3) > 0$ and $\lambda_1\lambda_2\lambda_3 = -a(1 - \frac{k_3d_3}{c}) > 0$, Eq. (29) has three positive eigenvalues, or one positive eigenvalue and two negative eigenvalues, or one positive eigenvalue and a pair of complex conjugate eigenvalues. Based on numerical observations, one may assume that Eq. (29) has one positive eigenvalue and a pair of complex conjugate eigenvalues with negative real parts. Thus, all equilibria in A_2 are *saddle points of index 1*. For all equilibria in A_3, the corresponding characteristic equations are (22). According to the assumption in the last subsection, the equilibria in A_3 are *saddle points of index 1*. For the equilibria in A_4, the corresponding characteristic equations are

$$\lambda^3 + (c - d_3k_3)\lambda^2 + (b - d_2k_2)\left(1 - \frac{k_3d_3}{c}\right)\lambda + a\left(1 - \frac{k_2d_2}{b}\right)\left(1 - \frac{k_3d_3}{c}\right) = 0. \tag{30}$$

Since $\lambda_1 + \lambda_2 + \lambda_3 = -(c - d_3k_3) > 0$ and $\lambda_1\lambda_2\lambda_3 = -a(1 - \frac{k_2d_2}{b})(1 - \frac{k_3d_3}{c}) < 0$, Eq. (30) has one negative eigenvalue and two positive eigenvalues, or one negative eigenvalue and a pair of complex conjugate eigenvalues with positive real parts. Our numerical observations show that Eq. (30) has one negative eigenvalue and a pair of conjugately complex eigenvalues with positive real parts. Thus, the equilibria in A_4 are *saddle points of index 2*. For all equilibria in A_5, the corresponding characteristic equations are (16). According to the assumption in Subsection B, all equilibria in A_5 are *saddle points of index 1*. For the equilibria in A_6, the corresponding characteristic equations are

$$\lambda^3 + (c - d_3k_3)\lambda^2 + b\left(1 - \frac{k_3d_3}{c}\right)\lambda + (a - k_1d_1)\left(1 - \frac{k_3d_3}{c}\right) = 0. \tag{31}$$

Since $\lambda_1 + \lambda_2 + \lambda_3 = -(c - d_3k_3) > 0$ and $\lambda_1\lambda_2\lambda_3 = -(a - k_1d_1)(1 - \frac{k_3d_3}{c}) < 0$, Eq. (31) has one negative eigenvalue and two positive eigenvalues, or one negative eigenvalue and a pair of complex conjugate eigenvalues with positive real parts. Our numerical simulations show that Eq. (31) has one negative eigenvalue and two positive eigenvalues. So the equilibria in A_6 are *saddle points of index 1*. For all equilibria in A_7, the corresponding characteristic equations are Eq. (23). From the assumption in the last subsection, all equilibria in A_7 are *saddle points of index 2*. Finally, for all equilibria in A_8, the corresponding characteristic equations are

$$\lambda^3 + (c - d_3k_3)\lambda^2 + (b - d_2k_2)\left(1 - \frac{k_3d_3}{c}\right)\lambda + (a - k_1d_1)\left(1 - \frac{k_2d_2}{b}\right)\left(1 - \frac{k_3d_3}{c}\right) = 0. \tag{32}$$

Since $\lambda_1 + \lambda_2 + \lambda_3 = -(c - d_3k_3) > 0$ and $\lambda_1\lambda_2\lambda_3 = -(a - d_1k_1)(1 - \frac{k_2d_2}{b})(1 - \frac{k_3d_3}{c}) > 0$, Eq. (32) has three positive eigenvalues, or one positive eigenvalue and two negative eigenvalues, or one positive eigenvalue and a pair of complex conjugate eigenvalues. Our numerical observations show that Eq. (32) has one positive eigenvalue and a pair of complex conjugate eigenvalues with negative real parts. Then, the equilibria in A_8 are *saddle points of index 1*.

It should be pointed out that the scrolls can be generated only around *saddle points of index 2* [16,17]. Therefore, only the equilibria in A_1, A_4, and A_7 may create scrolls. However, our numerical observations reveal that only the equilibria in A_1 can generate scrolls. In fact, having a *saddle point of index 2* is only a necessary condition, but not a sufficient condition for generating scrolls. That is, system (24) has the potential to create a maximum of 3D $(p_1 + q_1 + 2) \times (p_2 + q_2 + 2) \times (p_3 + q_3 + 2)-$grid scroll chaotic attractor, called *3-D $n \times m \times l-$grid scroll* chaotic attractor, for some suitable parameters $a, b, c, d_1, d_2, d_3, k_1, h_1, k_2, h_2, k_3, h_3$. Especially, each equilibrium point in A_1 corresponds to a unique 3D *saturated plateau* and also corresponds to a unique scroll in the whole attractor. Furthermore, other equilibria in $A_i\,(2 \le i \le 8)$ correspond to the *saturated slopes* and are responsible for connecting the $(p_1 + q_1 + 2) \times (p_2 + q_2 + 2) \times (p_3 + q_3 + 2)$ scrolls.

Figure 7 shows a $6 \times 6 \times 6-$grid scroll chaotic attractor, where $a = d_1 = 0.7$, $b = c = d_2 = d_3 = 0.8$, $k_1 = 100$, $h_1 = 200$, $k_2 = k_3 = 40$, $h_2 = h_3 = 80$, $p_1 = p_2 = p_3 = q_1 = q_2 = q_3 = 2$. Obviously, there are 6 scrolls in each direction of the state space, as shown in Figure 7 (a) and (b), respectively. The Lyapunov exponent spectrum of this $6 \times 6 \times 6-$grid scroll attractor includes $LE_1 = 0.0885$, $LE_2 = 0$, $LE_3 = -0.7157$. Note that these 3-D $n \times m \times l-$grid scroll chaotic attractors are generated in exactly the same way as the 1-D and 2-D cases discussed before, except that the directions of the system trajectories are three here.

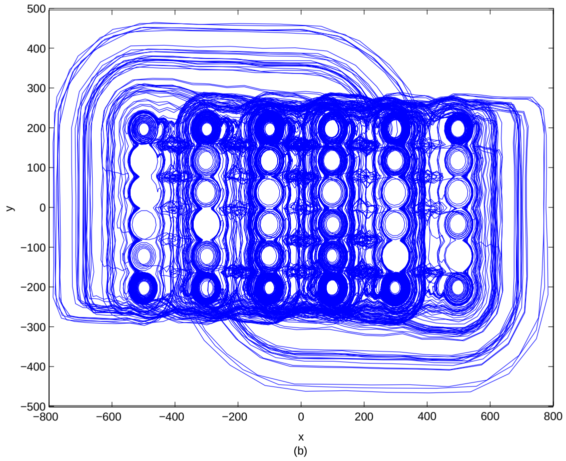

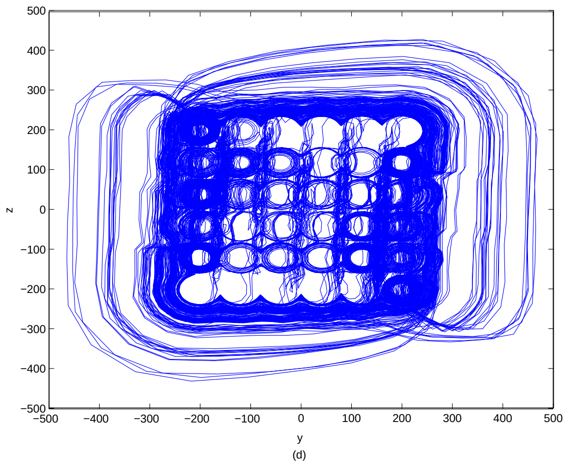

Figure 7. 3-D 6 × 6 × 6−grid scroll chaotic attractors. (a) x-y plane projection; (b) y-z plane projection.

4 Conclusions

This paper has proposed a switching control method — saturated function series approach — for generating multi-scroll chaotic attractors, including 1-D $n-$scroll, 2-D $n \times m-$grid scroll, and 3-D $n \times m \times l-$grid scroll attractors, from a given 3-D linear autonomous system with a saturated function series controller. The chaos generation mechanism of multi-scroll systems has also been briefly discussed by analyzing the system equilibria. It should be pointed out that one can arbitrarily design a desired number of scrolls and their spatial positions and orientations by using this developed systematic methodology. Moreover, it is relatively easy to design physical electronic circuits to experimentally verify these multi-scroll chaotic attractors since the saturated circuit is a basic electrical circuit. As one typical application, we recently have found that multi-scroll chaotic signals provide the best liquid mixing quality, which will be reported in a forthcoming paper. Various related bifurcation phenomena also deserve further investigation in the near future.

Acknowledgements

This work was supported by the Hong Kong Research Grants Council under the CERG grant CityU 1115/03E and the National Natural Science Foundation of China No. 60304017.

References

[1] G. Chen, and J. Lü, *Dynamics of the Lorenz System Family: Analysis, Control and Synchronization*, Science Press, Beijing, China, 2003.

[2] G. Chen, and X. Yu, (Eds) *Chaos Control: Theory and Applications*, Springer-Verlag, Berlin, Heidelberg, 2003.

[3] J. A. K. Suykens, and J. Vandewalle, *Generation of $n-$double scrolls (n = 1, 2, 3, 4, $\cdots$)*, IEEE Trans. Circuits Syst. I, Vol. 40, No. 11, pp. 861-867, Nov. 1993.

[4] J. A. K. Suykens, A. Huang, and L. O. Chua, *A family of $n-$scroll attractors from a generalized Chua's circuit*, Int. J. Electron. Commun., Vol. 51, No. 3, pp. 131-138, 1997.

[5] J. A. K. Suykens, and L. O. Chua, *$n-$double scroll hypercubes in 1-D CNNs*, Int. J. Bifurcation Chaos, Vol. 7, No. 8, pp. 1873-1885, 1997.

[6] M. E. Yalcin, S. Ozoguz, J. A. K. Suykens, and J. Vandewalle, *n-scroll chaos generators: a simple circuit model*, Electronics Letters, Vol. 37, No. 3, pp. 147-148, 2001.

[7] K. S. Tang, G. Q. Zhong, G. Chen, and K. F. Man, *Generation of $n-$scroll attractors via sine function*, IEEE Trans. Circuits Syst. I, Vol. 48, pp. 1369-1372, Nov. 2001.

[8] M. E. Yalcin, S. Ozoguz, J. A. K. Suykens, and J. Vandewalle, *Scroll maps from n-scroll attractors*, The 10 th workshop on nonlinear dynamics of electronic systems, Vol. 2, pp. 45-48, 21-23 June 2002, Izmir, Turkey.

[9] M. E. Yalcin, J. A. K. Suykens, J. Vandewalle, and S. Ozoguz, *Families of scroll grid attractors*, Int. J. Bifurcation Chaos, Vol. 12, No. 1, pp. 23-41, Jan. 2002.

[10] S. Ozoguz, A. S. Elwakil, and K. N. Salama, *n-scroll chaos generator using nonlinear transconductor*, Electronics Letters, Vol. 38, pp. 685-686, 2002.

[11] G. Zhong, K. F. Man, and G. Chen, *A systematic approach to generating $n-$scroll attractors*, Int. J. Bifurcation Chaos, Vol. 12, No. 12, pp. 2907-2915, Dec. 2002.

[12] J. Lü, T. Zhou, G. Chen, and X. Yang, *Generating chaos with a switching piecewise-linear controller*, Chaos, Vol. 12, No. 2, pp. 344-349, 2002.

[13] J. Lü, X. Yu, and G. Chen, *Generating chaotic attractors with multiple merged basins of attraction: A switching piecewise-linear control approach*, IEEE Trans. Circuits Syst. I, Vol. 50, pp. 198-207, Feb. 2003.

[14] F. Han, J. Lü, X. Yu, G. Chen, and Y. Feng, *A new systematic method for generating multi-scroll chaotic attractors from a linear second-order system with hysteresis*, Int. J. Bifurcation Chaos, 2004, in press.

[15] J. Lü, F. Han, X. Yu, and G. Chen, *Generating 3-D multi-scroll chaotic attractors: A hysteresis series switching method*, Automatica, 2004, in press.

[16] D. Cafagna, and G. Grassi, *New 3D-scroll attractors in hyperchaotic Chua's circuit forming a ring*, Int. J. Bifurcation Chaos, Vol. 13, No. 10, pp. 2889-2903, 2003.

[17] L. O. Chua, M. Komuro, and T. Matsumoto, *The double scroll family*, IEEE Trans. Circuits Syst. I, Vol. 33, pp. 1072-1118, Nov. 1986.

[18] C. P. Silva, *Shil'nikov's theorem — a tutorial*, IEEE Trans. Circuits Syst. I, Vol. 40, pp. 675-682, Oct. 1993.

[19] A. S. Elwakil, K. N. Salama, and M. P. Kennedy, *A system for chaos generation and its implementation in monolithic form*, Proceedings of the IEEE Symp. Circuits Syst. ISCAS'00, pp. 217-220, Geneva, 2000.

[20] A. S. Elwakil, and M. P. Kennedy, *Construction of classes of circuit-independent chaotic oscillators using passive-only nonlinear devices*, IEEE Trans. Circuits Syst. I, Vol. 48, pp. 289-307, 2001.

[21] T. Saito, and S. Nakagawa, *Chaos from a hysteresis and switched circuit*, Phil. Trans. R. Soc. Lond. A, Vol. 353, pp. 47-57, 1995.

[22] S. Nakagawa, and T. Saito, *An RC OTA hysteresis chaos generator*, IEEE Trans. Circuits Syst. I, Vol. 43, pp. 1019-1021, Dec. 1996.

[23] A. S. Kennedy, and M. P. Kennedy, *Chaotic oscillators derived from Saito's double-screw hysteresis oscillator*, IEICE Trans. Fundamentals, Vol. E82, pp. 1769-1775, 1999.

[24] A. S. Elwakil, and M. P. Kennedy, *Systematic realization of a class of hysteresis chaotic oscillators*, Int. J. Circuit Theor. Appl., Vol. 28, pp. 319-334, 2000.

[25] M. Storace, M. Parodi, and D. Robatto, *A hysteresis-based chaotic circuit: dynamics and applications*, Int. J. Circuit Theory Applications, Vol. 27, pp. 427-542, 1999.

[26] J. Vandewalle, and L. Vandenberghe, *Piecewise-linear circuits and piecewise-linear analysis*, in W. K. Chen, (Ed.) The Circuits and Filters Handbook, CRC Press and IEEE Press, USA, 1995, pp. 1034-1057.

[27] J. Lü, J. Lu, and S. Chen, *Chaotic Time Series Analysis and Its Applications*, Wuhan University Press, China, 2002.